

# Array Geometry-Robust Attention-Based Neural Beamformer for Moving Speakers

Marvin Tammen<sup>1,2</sup>, Tsubasa Ochiai<sup>1</sup>, Marc Delcroix<sup>1</sup>, Tomohiro Nakatani<sup>1</sup>, Shoko Araki<sup>1</sup>, Simon Doclo<sup>2</sup>

<sup>1</sup>NTT Corporation, Japan

<sup>2</sup>Carl von Ossietzky Universität Oldenburg, Germany

marvin.tammen@uol.de

## Abstract

Recently, a mask-based beamformer with attention-based spatial covariance matrix aggregator (ASA) was proposed, which was demonstrated to track moving sources accurately. However, the deep neural network model used in this algorithm is limited to a specific channel configuration, requiring a different model in case a different channel permutation, channel count, or microphone array geometry is considered. Addressing this limitation, in this paper, we investigate three approaches to improve the robustness of the ASA-based tracking method against such variations: incorporating random channel configurations during the training process, employing the transform-average-concatenate (TAC) method to process multi-channel input features (allowing for any channel count and enabling permutation invariance), and utilizing input features that are robust against variations of the channel configuration. Our experiments, conducted using the CHiME-3 and DEMAND datasets, demonstrate improved robustness against mismatches in channel permutations, channel counts, and microphone array geometries compared to the conventional ASA-based tracking method without compromising performance in matched conditions, suggesting that the mask-based beamformer with ASA integrating the proposed approaches has the potential to track moving sources for arbitrary microphone arrays.

**Index Terms:** multi-channel speech enhancement, moving speaker, mask-based beamformer, array geometry-robust processing

## 1. Introduction

In many speech communication scenarios, a prevalent issue is the corruption of microphone signals by noise, reducing speech quality and intelligibility as well as degrading the performance of automatic speech recognition (ASR) systems. When multiple microphones are available, an effective solution to this issue lies in the use of beamformers [1]. Beamformers typically yield a good speech enhancement performance with low speech distortion, provided that accurate estimates of the required spatial covariance matrices (SCMs) are available.

In mask-based beamformers, this estimation task has often been offloaded to deep neural networks (DNNs) [2–11], demonstrating a remarkable performance in recent ASR challenges [12] while typically being applicable to arbitrary channel configurations, i.e., the permutation and count of channels as well as the associated microphone array geometry. However, most studies have focused on stationary acoustic scenes, where the SCMs were estimated by averaging across entire utterances [2, 4, 6, 9]. This approach falls short in realistic acoustic scenarios involving moving sources, where the SCMs are inherently time-varying and require temporal adaptation or tracking. Traditionally, various heuristic tracking methods, such as block-online estimation or recursive smoothing, have been employed [5]. While potentially effective, these methods rely heavily on the manual tuning of parameters such as smoothing factors, which can vary according to the acoustic scenario.

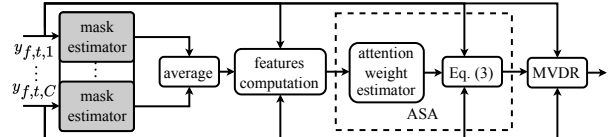


Figure 1: Overview of mask-based MVDR beamformer with ASA. Grey vertically stacked boxes share weights.

To avoid the manual tuning of such parameters, a mask-based beamformer employing an attention-based SCM aggregator (ASA) was proposed in [11]. The ASA temporally aggregates instantaneous estimates of the SCMs to estimate the speech and noise SCMs used to implement a time-varying beamformer. In [11], the ASA was demonstrated to accurately track sources, outperforming the baseline heuristic tracking methods. By employing a training process, a DNN architecture, and input features that were dependent on the channel configuration, the ASA lost one of the key benefits of conventional mask-based beamformers. However, as discussed in Section 2.3, the ASA itself does not depend on the channel configuration.

Hence, in this paper, we propose three approaches extending the prior work in [11] with the goal of realizing a mask-based beamformer with ASA that exhibits robustness against variations of the channel configuration and is thus capable of tracking moving sources for arbitrary microphone arrays. First, we investigate incorporating random channel configurations in the training process for preventing the DNN from overfitting to specific channel permutations and channel counts. The transform-average-concatenate (TAC) method was originally proposed to enable the FaSNet algorithm to perform channel permutation-invariant multi-channel source separation [13] and has been successfully employed in various algorithms, including time-frequency masking algorithms [14, 15] and stationary mask-based beamformers [9]. Third, we investigate utilizing different input features that are less sensitive to variations of the channel configuration than the input features in [11]. Through experiments conducted using the CHiME-3 [12] and DEMAND [16] datasets, we demonstrate the benefit of jointly integrating the three proposed approaches in the ASA. Notably, our proposed approaches not only yield a good speech enhancement performance even for microphone arrays unseen during training, but also maintain high performance under matched conditions.

## 2. Conventional: Mask-Based Beamformer with Attention-Based Spatial Covariance Matrix Aggregator

In this section, we provide an overview of the mask-based beamformer with ASA, as proposed in [11] (see Fig. 1 for a schematic representation).

## 2.1. MVDR Beamformer

We consider an acoustic scenario with a single moving speech source and additive noise, located in a reverberant room and recorded by a set of  $C$  microphones. In the short-time Fourier transform (STFT) domain, the vector comprising the  $C$  noisy microphone signals can be written as  $\mathbf{y}_{f,t} = [y_{f,t,c=1} \dots y_{f,t,c=C}]^T \in \mathbb{C}^C$ , with  $f$ ,  $t$ , and  $c$  denoting the frequency bin index, the time frame index, and the channel index, respectively, and with  $\cdot^T$  denoting the transpose operator. Assuming that the (time-varying) acoustic transfer function between the source and the microphones is shorter than the STFT frame length, the noisy vector can be written as  $\mathbf{y}_{f,t} = \mathbf{h}_{f,t} s_{f,t} + \mathbf{n}_{f,t}$ , where  $\mathbf{h}_{f,t} \in \mathbb{C}^C$ ,  $s_{f,t} \in \mathbb{C}$ , and  $\mathbf{n}_{f,t} \in \mathbb{C}^C$  denote the (time-varying) acoustic transfer function, the speech source, and the additive noise component, respectively.

In beamforming approaches, the target speech component  $x_{f,t,r} = h_{f,t,r} s_{f,t}$  at a reference microphone  $c = r$  is typically estimated by applying a linear filter  $\mathbf{w}_{f,t} \in \mathbb{C}^C$  to the noisy vector as:

$$\hat{x}_{f,t,r} = \mathbf{w}_{f,t}^H \mathbf{y}_{f,t}, \quad (1)$$

where  $\cdot^H$  denotes the conjugate transpose operator. Aiming at minimizing the output noise power spectral density while leaving the target speech component undistorted, the minimum variance distortionless response (MVDR) beamformer filter vector can be derived as [17]:

$$\mathbf{w}_{f,t} = \frac{(\Phi_{f,t}^n)^{-1} \Phi_{f,t}^x}{\text{tr}((\Phi_{f,t}^n)^{-1} \Phi_{f,t}^x)} \mathbf{u}_r, \quad (2)$$

where  $\Phi_{f,t}^x \in \mathbb{C}^{C \times C}$  and  $\Phi_{f,t}^n \in \mathbb{C}^{C \times C}$  denote the speech and noise SCMs, respectively,  $\text{tr}(\cdot)$  denotes the trace operator, and  $\mathbf{u}_r \in \{0,1\}^C$  denotes a selection vector with a 1 as the  $r$ -th element and 0 otherwise.

## 2.2. Spatial Covariance Matrix Estimation

To implement the MVDR beamformer in Eq. (2), estimates of the speech and noise SCMs ( $\Phi_{f,t}^x$  and  $\Phi_{f,t}^n$ ) are required. Allowing for a time-varying estimation of  $\Phi_{f,t}^x$ , the previous study [11] extended the mask-based beamformer formulation proposed in [2] by introducing the following SCM temporal aggregation mechanism:

$$\hat{\Phi}_{f,t}^\nu = \sum_{t'=1}^T a_{t,t'}^\nu \underbrace{m_{f,t'}^\nu \mathbf{y}_{f,t'} \mathbf{y}_{f,t'}^H}_{=\hat{\Psi}_{f,t'}^\nu} \quad (3)$$

$$\mathbf{a}_t^\nu = [a_{t,t'=1}^\nu \dots a_{t,t'=T}^\nu]^T \in \mathbb{R}^T, \quad (4)$$

where  $\nu \in \{x,n\}$  denotes the speech or noise component,  $m_{f,t}^\nu$  denotes a time-frequency mask,  $\hat{\Psi}_{f,t}^\nu \in \mathbb{C}^{C \times C}$  can be interpreted as an instantaneous SCM (ISCM) estimate, and  $T$  denotes the number of time frames. The (frequency-independent) so-called attention weights  $\mathbf{a}_t^\nu$  control how the ISCM estimates are temporally aggregated to yield estimates of the speech or noise SCM at the  $t$ -th time frame.

## 2.3. Attention Weight Estimation

To obtain the attention weights for the temporal aggregation of the speech and noise SCMs in the ASA, a self-attention-based DNN (i.e., a Transformer encoder [18]) is adopted as:

$$\{\mathbf{a}_t\}_{t=1}^T = \text{DNN}(\{\mathbf{i}_t\}_{t=1}^T; \mathbf{\Lambda}), \quad (5)$$

where  $\mathbf{a}_t = [a_{t,t=1}^x \dots a_{t,t=T}^x]^T$ ,  $\mathbf{i}_t = [i_{t,t=1}^x \dots i_{t,t=T}^x]^T$ ,  $\mathbf{i}_t^\nu$  denotes the input features at time frame  $t$ , and  $\mathbf{\Lambda}$  denotes the parameters of the DNN.<sup>1</sup> As illustrated in Fig. 2a, first, the input features are transformed

<sup>1</sup>In [11], two dedicated DNNs  $\text{DNN}^x(\cdot)$  and  $\text{DNN}^n(\cdot)$  for the speech and noise components were used. Our preliminary experiments showed a similar or better performance at a lower computational complexity when using a single DNN.

into a time-varying embedding vector via a feedforward layer. This embedding vector then passes through several multi-head attention (MHA) encoder blocks, each comprising multi-head self-attention layers and position-wise feedforward layers, all interconnected through residual connections. Finally, the attention weights  $\{\mathbf{a}_t\}_{t=1}^T$  are extracted from the final (single-head attention) encoder block.

The speech and noise features  $\mathbf{i}_t^\nu$  are based on the ISCMs defined in Eq. (3), i.e.,

$$\mathbf{i}_{f,t}^{\nu, \text{ISCM}} = \left[ \Re(\text{Vec}(\hat{\Psi}_{f,t}^\nu)^T) \Im(\text{Vec}(\hat{\Psi}_{f,t}^\nu)^T) \right]^T \in \mathbb{R}^{2C^2}, \quad (6)$$

where  $\text{Vec}(\cdot)$  denotes a reshaping of a  $C \times C$ -dimensional matrix as a vector of length  $C^2$ .

As described in Section 2.2, the attention weights  $\{\mathbf{a}_t\}_{t=1}^T$  control the temporal aggregation of the speech and noise SCMs. Crucially, in this formulation, the attention weights are not dependent on the channel configuration, in particular allowing for a potential application across varied microphone arrays. However, due to the used training process, the design of its DNN architecture, as well as the used input features, the approach proposed in [11] does depend on the channel configuration. More specifically, the training process did not account for channel configuration variability, using instead a fixed channel configuration, and the DNN architecture had a fixed input layer size. Furthermore, the ISCM-based features in Eq. (6) simultaneously incorporate spatial and spectro-temporal information, making them sensitive to the channel configuration observed during training.

## 3. Proposed: Improving Robustness Against Channel Configuration Variations

In this paper, to increase the robustness of the mask-based beamformer with ASA against variations of the channel configuration, we investigate three approaches: 1) using a training procedure that incorporates random channel configurations, 2) employing TAC to process multi-channel features (allowing for any channel count and enabling permutation invariance), and 3) choosing features that are robust against variations of the channel configuration.

### 3.1. Training With Random Channel Configurations

To enhance the robustness of the ASA against channel configuration variations, we propose integrating random channel configurations into the training process. More explicitly, for each minibatch, a channel count  $C' \sim \mathcal{U}(2, C_{\max})$  is drawn randomly, where  $\mathcal{U}$  denotes the uniform random distribution and  $C_{\max}$  denotes the maximum channel count observed during training. From the available  $C_{\max}$  channels,  $C'$  channels are then selected in random permutation. While this approach is simple, it is essential to prevent the DNN from overfitting to specific channel permutations, channel counts, and microphone array geometries, thereby extracting more robust features.

### 3.2. Employing TAC to Process Multi-Channel Features

To accommodate a variable number of input channels in the training of the DNN with fixed input layer size, we can apply zero-padding up to  $C_{\max}$  channels. It can be expected that this approach sacrifices performance for robustness, since the DNN needs to learn to deal with zero-padded input features, while also being restricted to  $C_{\max}$  or fewer channels.

To deal with these issues, we propose to employ the TAC method [13] to process multi-channel features in the attention weight estimator as depicted in Fig. 2c. The integration is achieved by interleaving TAC blocks with parallel MHA encoder blocks sharing the same parameters. After  $N'$  stacks of parallel interleaved TAC blocks and MHA encoder blocks, the streams are averaged, followed

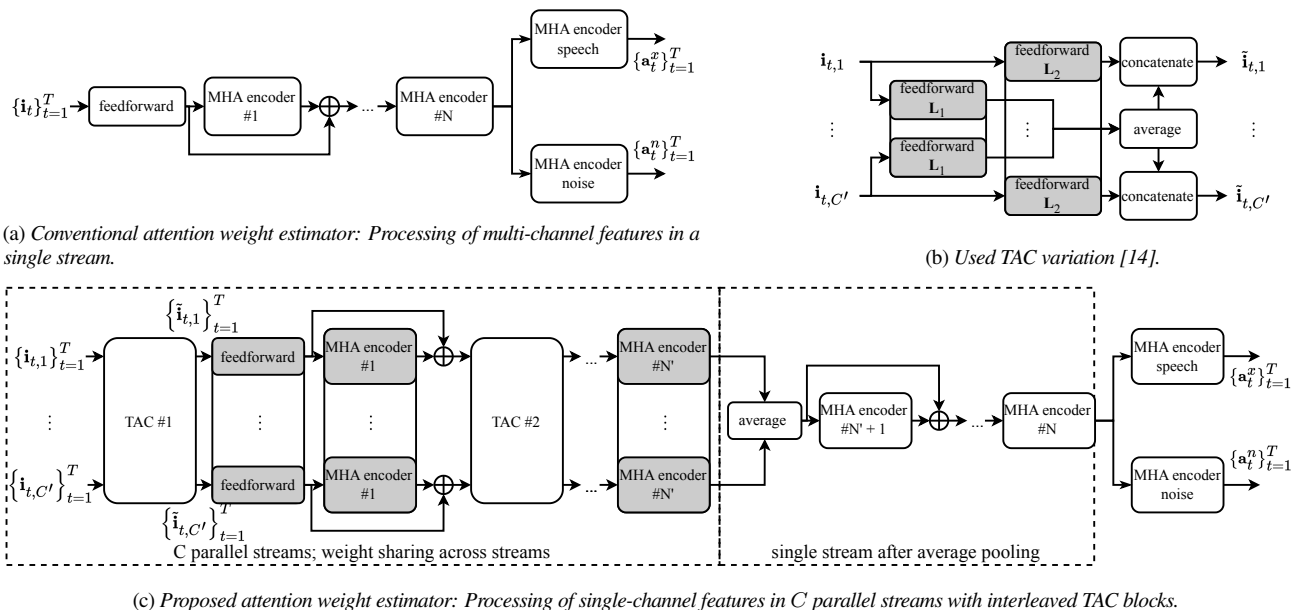


Figure 2: Attention weight estimator employing different approaches to integrate multi-channel features and visualization of the used TAC variation.

by  $N - N'$  further single-stream MHA encoder blocks.

A TAC block takes as input a variable-sized set of feature streams  $\{\mathbf{i}_{t,c} \in \mathbb{R}^D\}_{c=1}^{C'}$  with (channel-independent) feature dimension  $D$ , shares information across the streams in a non-linearly transformed space, and outputs a set of modified feature streams  $\{\tilde{\mathbf{i}}_{t,c} \in \mathbb{R}^D\}_{c=1}^{C'}$  (see Fig. 2b). More specifically, we adopt the efficient TAC implementation from [14], obtaining the modified feature stream at time frame  $t$  and channel  $c$  as:

$$\tilde{\mathbf{i}}_{t,c} = \left[ \text{ReLU}(\mathbf{L}_1 \mathbf{i}_{t,c})^\top \quad \frac{1}{C'} \sum_{\mu=1}^{C'} \text{ReLU}(\mathbf{L}_2 \mathbf{i}_{t,\mu})^\top \right]^\top, \quad (7)$$

where  $\mathbf{L}_1$  and  $\mathbf{L}_2$  denote  $((D/2) \times D)$ -dimensional trainable linear transforms. Notably, the modified feature streams contain channel-specific information as well as information affected by all channels in a permutation-invariant fashion due to the combination of weight sharing and the application of the permutation-invariant average operation.

This integration of the TAC method provides two main benefits to the attention weight estimator: First, it enables handling a varying channel count  $C'$  and second, it ensures invariance to the channel permutation. These benefits significantly enhance the flexibility and applicability of the attention weight estimator across diverse channel configurations, without necessitating modifications in the DNN architecture or hyperparameters.

### 3.3. Input Features

The previous study [11] adopted the vectorized speech and noise ISCM-based features defined in Eq. (6), both concatenated along the frequency dimension to result in  $\mathbf{i}_t^{\text{ISCM}} \in \mathbb{R}^{4FC^2}$ , as the input features of the DNN. Due to the definition of the ISCM, these features depend on the channel pairs, simultaneously encoding inter-microphone level differences (ILDs) as well as inter-microphone phase differences (IPDs), which strongly depend on inter-microphone distances. In addition, the TAC method requires channel-wise feature streams with a channel count-independent feature dimension, and thus the  $4FC^2$ -dimensional features  $\mathbf{i}_t^{\text{ISCM}}$  in Eq. (6) are incompatible with the TAC method.

In this paper, to address these issues, we investigate adopting alternative channel-wise feature streams  $\mathbf{i}_{f,t,c}^{\nu, \text{mag-IPD}}$  based on the squared masked magnitude spectra and the IPDs relative to the channel-averaged masked STFT coefficients as:

$$\mathbf{i}_{f,t,c}^{\nu, \text{mag-IPD}} = \left[ |\hat{\nu}_{f,t,c}|^2, \angle \hat{\nu}_{f,t,c} - \angle \hat{\sigma}_{f,t} \right]^\top, \quad (8)$$

where  $\hat{\nu}_{f,t,c} = m_{f,t}^\nu y_{f,t,c}$  denotes the masked STFT coefficients,  $\angle \cdot$  denotes the (wrapped) phase of  $\cdot$ , and  $\hat{\sigma}_{f,t} = \frac{1}{C} \sum_{c=1}^C \hat{\nu}_{f,t,c}$  denotes the channel-averaged masked STFT coefficients. Concatenating the speech and noise features along the frequency dimension yields  $C$  streams of  $4F$ -dimensional features  $\mathbf{i}_{t,c}^{\text{mag-IPD, TAC}}$ . We hypothesize that these features are less sensitive to variations of the channel configuration than the features in Eq. (6) because first, they do not explicitly depend on channel pairs and second, they effectively separate the channel configuration-dependent IPD information from magnitude information, which is less influenced by channel configurations. Preliminary simulations showed a benefit of using channel-wise squared magnitude spectra instead of the channel-averaged masked magnitude spectrum as in [14]. To evaluate the influence of replacing the ISCM-based features with the mag-IPD-based features without employing the TAC method, we also utilize the mag-IPD-based features with the conventional ASA, concatenating the speech and noise features along the frequency and channel dimensions, yielding  $4FC$ -dimensional features  $\mathbf{i}_t^{\text{mag-IPD, cat}}$ .

## 4. Experiments

### 4.1. Datasets

To evaluate the effectiveness of the proposed approaches, we constructed datasets of simulated moving sources in noisy conditions using speech recordings from the Wall Street Journal (WSJ0) corpus [19] and noise recordings from the CHiME-3 [12] and DEMAND [16] corpora. Similarly as in [11], we simulated sources moving on a linear trajectory with constant speed using the gprIR tool [20] by generating room impulse responses (RIRs) at 128 positions on a line, with room widths and depths uniformly drawn from 3.0 m, 3.5 m, 4.0 m, 4.5 m and 5.0 m, the room height equal to 2.5 m, reverberation times  $T_{60}$  between 0.1 s and 0.3 s, and with

		config.	features	use TAC	matched		mismatched in terms of							
					PESQ	SDR	Permutation		Count		Geometry		Count & Geom.	
							PESQ	SDR	PESQ	SDR	PESQ	SDR	PESQ	SDR
1	baseline	fixed	ISCM	False	<b>2.64</b>	16.34	2.31	13.72	1.84	10.66	2.19	11.32	1.71	7.39
2	proposed	fixed	mag-ipd	False	2.57	16.27	2.40	14.70	1.84	10.71	2.15	11.01	1.77	8.34
3	proposed	fixed	mag-ipd	True	2.62	<b>16.39</b>	<b>2.62</b>	<b>16.39</b>	2.05	12.55	2.20	11.84	1.87	9.25
4	proposed	random	ISCM	False	2.42	14.37	2.42	14.36	1.96	11.86	2.18	11.55	1.93	10.02
5	proposed	random	mag-ipd	False	2.53	15.85	2.52	15.86	2.32	14.07	2.18	11.82	1.99	10.54
6	proposed	random	mag-ipd	True	2.59	16.02	2.59	16.02	<b>2.34</b>	<b>14.15</b>	<b>2.21</b>	<b>12.35</b>	<b>2.03</b>	<b>11.34</b>

Table 1: Mean PESQ and SDR values for the mask-based MVDR beamformer with ASA employing different attention weight estimators, evaluated on datasets corresponding to a matched condition and various mismatched conditions.



Figure 3: Microphone array geometries used in the CHiME-based and DEMAND-based datasets. Grey circles denote the reference microphone and white circles denote unused microphones.

the microphone array randomly placed in the room. We added the source signal convolved with the simulated RIRs and the recorded noise signals at signal-to-noise-ratios (SNRs) between 2 dB and 8 dB.

We constructed two datasets with different microphone array geometries, illustrated in Fig. 3. First, we generated simulated utterances based on the WSJ0 speech and CHiME-3 noise signals and used this dataset for training, development, and evaluation, resulting in a maximum number of  $C_{\max} = 5$  channels (excluding the rear-facing second channel). Second, we generated simulated utterances based on the WSJ0 speech and DEMAND noise signals and used this dataset for evaluation, resulting in a maximum number of 16 channels.

To evaluate a mismatch in terms of the channel permutation, we randomly permuted the channels from the CHiME-3-based evaluation dataset, while always keeping the same microphone as the reference channel (see. Fig. 3a). To evaluate a mismatch in terms of the channel count, we selected the first  $C = 3$  channels from the CHiME-3-based evaluation dataset. To evaluate a mismatch in terms of the microphone array geometry, we randomly selected  $C = 5$  channels from the DEMAND-based evaluation dataset, while always keeping the same microphone as the reference channel (see. Fig. 3b). This procedure allows for diverse microphone array geometries including, e.g., linear, triangular, rectangular and trapezoidal shapes (see. Fig. 3b). To evaluate a mismatch in terms of both the channel count and the microphone array geometry, we randomly selected  $C = 3$  channels from the DEMAND-based evaluation dataset. We created 30000, 2000, and 2000 noisy speech signals for training, development, and each evaluation dataset, respectively.

## 4.2. Settings

We followed the experimental settings in [11] to increase comparability with the associated results. We trained the attention weight estimator in an end-to-end manner, utilizing the scale-dependent SNR loss function [21] at the output of the mask-based beamformer (see Fig. 1), with the reverberant clean speech at the reference microphone

as the target signal. During training, we used oracle “Wiener-like” time-frequency masks [22] to compute the ISCMs and optimized only the parameters of the attention weight estimator. During evaluation, we used estimated time-frequency masks obtained with a time-frequency mask estimator based on a temporal convolutional network architecture [23]. For the attention weight and time-frequency mask estimators, we adopted the DNN and training hyperparameters in [11] and set  $N' = 2$ . For the TAC module, we adopted the modified implementation proposed in [14], with the feedforward blocks consisting of a linear layer and a ReLU activation (Eq. (7)). For the STFT, a Hann window with a frame length of 64 ms and 16 ms shift was used. Speech enhancement performance was evaluated in terms of perceptual evaluation of speech quality (PESQ) [24] and signal-to-distortion-ratio (SDR) [25] (allowing for distortions caused by time-invariant filters), with the reverberant clean speech at the reference microphone chosen as the reference signal.

## 4.3. Results

Table 1 shows the speech enhancement performance in terms of PESQ and SDR for the mask-based beamformer with ASA employing different attention weight estimators, indexed by the left-most column. In this table, “config” represents whether the channel permutation and count were randomized during training as described in Section 3.1 or fixed; “features” represents the utilized input feature (ISCM-based in Eq. (6) or mag-IPD-based in Eq. (8)); and “use TAC” represents whether TAC was employed (Fig. 2c) or not (Fig. 2a). We evaluated these estimators under a matched condition and various mismatched conditions described in Section 4.1. “matched” represents the evaluation dataset with a fixed channel permutation, the channel count  $C = C_{\max} = 5$ , as well as the CHiME-3 microphone array geometry, which matches the fixed training condition. The mismatched evaluation datasets include variations in the channel permutation (random), the channel count ( $C = 3$ ), the microphone array geometry (DEMAND), as well as the channel count and microphone array geometry ( $C = 3$  and DEMAND).

From the table, we can observe that under the matched condition ( $C = 5$ , fixed channel permutation, CHiME-3 microphone array geometry), models trained with a fixed channel configuration (rows 1-3) achieved the highest PESQ and SDR scores. This is expected as these models can exploit the specific spatial information confronted with during the training setup, representing an upper bound in performance. When evaluating the baseline model (row 1) under mismatched conditions in terms of the channel permutation or particularly the channel count, a noticeable performance drop can be observed. The performance drop under the channel permutation mismatch condition was somewhat mitigated by using the mag-IPD features instead of the ISCM features (row 2) or by training with random channel configurations (row 4), albeit at a slight cost to matched condition performance.

Furthermore, the employment of the TAC method demonstrated its strength under these mismatched conditions, especially when combined with training with random channel configurations (rows 3, 6). This combination not only removed the performance degradation seen under the channel permutation mismatch condition, but also showed higher robustness to the channel count mismatch condition, while maintaining high performance under the matched condition.

Particularly under the mismatched conditions in terms of the channel count and the microphone array geometry, we can confirm that the combination of training with random channel configurations, employing the TAC method, and using the mag-IPD-based input features contributed to a higher speech enhancement performance, reinforcing the trend seen under the other mismatched conditions. It should be emphasized that this evaluation condition includes diverse microphone array geometries by randomly selecting channels from the DEMAND-based evaluation dataset. Hence, these results suggest that the mask-based beamformer with ASA employing the training with random channel configurations, the TAC method, and the mag-IPD features has the potential to track moving sources for arbitrary microphone arrays.

## 5. Conclusion

In this paper, we proposed several approaches to improve the robustness of the mask-based beamformer with ASA against channel configuration variations. These approaches include the incorporation of random channel configurations in the training procedure, employing the TAC method to process multi-channel features (allowing for any channel count and enabling permutation invariance), as well as using input features that are robust against variations of the channel configuration. Experiments conducted using the CHiME-3 and DEMAND datasets suggest that the mask-based beamformer with ASA integrating the proposed approaches has the potential to track moving sources for arbitrary microphone arrays. Future research will extend this investigation to further explore microphone array geometry-independent mask-based beamformers with ASA by dynamically generating diverse training data.

## 6. References

- [1] S. Doclo, W. Kellermann, S. Makino, and S. E. Nordholm, "Multichannel Signal Enhancement Algorithms for Assisted Listening Devices: Exploiting Spatial Diversity Using Multiple Microphones," *IEEE Signal Processing Magazine*, vol. 32, no. 2, pp. 18–30, Mar. 2015.
- [2] J. Heymann, L. Drude, and R. Haeb-Umbach, "Neural network based spectral mask estimation for acoustic beamforming," in *Proc. IEEE International Conference on Acoustics, Speech and Signal Processing (ICASSP)*, Shanghai, China, Mar. 2016, pp. 196–200.
- [3] T. Higuchi, N. Ito, T. Yoshioka, and T. Nakatani, "Robust MVDR beamforming using time-frequency masks for online/offline ASR in noise," in *Proc. IEEE International Conference on Acoustics, Speech and Signal Processing (ICASSP)*, Shanghai, China, Mar. 2016, pp. 5210–5214.
- [4] H. Erdogan, J. R. Hershey, S. Watanabe, M. I. Mandel, and J. L. Roux, "Improved MVDR Beamforming Using Single-Channel Mask Prediction Networks," in *Interspeech 2016*, San Francisco, CA, USA, Sep. 2016, pp. 1981–1985.
- [5] C. Boeddeker, H. Erdogan, T. Yoshioka, and R. Haeb-Umbach, "Exploring Practical Aspects of Neural Mask-Based Beamforming for Far-Field Speech Recognition," in *Proc. IEEE International Conference on Acoustics, Speech and Signal Processing (ICASSP)*, Calgary, Canada, Apr. 2018, pp. 6697–6701.
- [6] Z.-Q. Wang, P. Wang, and D. Wang, "Multi-microphone Complex Spectral Mapping for Utterance-wise and Continuous Speech Separation," *IEEE/ACM Transactions on Audio, Speech, and Language Processing*, vol. 29, pp. 2001–2014, 2021.
- [7] J. Casebeer, J. Donley, D. Wong, B. Xu, and A. Kumar, "NICE-Beam: Neural Integrated Covariance Estimators for Time-Varying Beamformers," Dec. 2021.
- [8] Y. Wang, A. Politis, and T. Virtanen, "Attention-Driven Multichannel Speech Enhancement in Moving Sound Source Scenarios," Dec. 2023.
- [9] A. Jukić, J. Balam, and B. Ginsburg, "Flexible Multichannel Speech Enhancement for Noise-Robust Frontend," in *Proc. IEEE Workshop on Applications of Signal Processing to Audio and Acoustics (WASPAA)*, New Paltz, NY, USA, Oct. 2023, pp. 1–5.
- [10] M. Tammen and S. Doclo, "Parameter Estimation Procedures for Deep Multi-Frame MVDR Filtering for Single-Microphone Speech Enhancement," *IEEE/ACM Transactions on Audio, Speech, and Language Processing*, vol. 31, pp. 1–13, Aug. 2023.
- [11] T. Ochiai, M. Delcroix, T. Nakatani, and S. Araki, "Mask-Based Neural Beamforming for Moving Speakers With Self-Attention-Based Tracking," *IEEE/ACM Transactions on Audio, Speech, and Language Processing*, vol. 31, pp. 835–848, 2023.
- [12] J. Barker, R. Marxer, E. Vincent, and S. Watanabe, "The third 'CHiME' speech separation and recognition challenge: Dataset, task and baselines," in *Proc. IEEE Workshop on Automatic Speech Recognition and Understanding (ASRU)*, Scottsdale, USA, Dec. 2015, pp. 504–511.
- [13] Y. Luo, Z. Chen, N. Mesgarani, and T. Yoshioka, "End-to-end Microphone Permutation and Number Invariant Multi-channel Speech Separation," *arXiv:1910.14104 [cs, eess]*, Nov. 2019.
- [14] T. Yoshioka, X. Wang, D. Wang, M. Tang, Z. Zhu, Z. Chen, and N. Kanda, "VarArray: Array-Geometry-Agnostic Continuous Speech Separation," in *Proc. IEEE International Conference on Acoustics, Speech and Signal Processing (ICASSP)*, May 2022, pp. 6027–6031.
- [15] D. Wang, Z. Chen, and T. Yoshioka, "Neural Speech Separation Using Spatially Distributed Microphones," in *Proc. Interspeech 2020*, Shanghai, China: ISCA, Oct. 2020, pp. 339–343.
- [16] J. Thiemann, N. Ito, and E. Vincent, "The Diverse Environments Multi-channel Acoustic Noise Database (DEMAND): A database of multichannel environmental noise recordings," in *Proc. Meetings on Acoustics (ICA)*, Montreal, Canada, 2013, pp. 1–6.
- [17] M. Souden, J. Benesty, and S. Affes, "On Optimal Frequency-Domain Multichannel Linear Filtering for Noise Reduction," *IEEE Transactions on Audio, Speech, and Language Processing*, vol. 18, no. 2, pp. 260–276, Feb. 2010.
- [18] A. Vaswani, N. Shazeer, N. Parmar, J. Uszkoreit, L. Jones, A. N. Gomez, L. Kaiser, and I. Polosukhin, "Attention is All you Need," in *Proc. Advances in Neural Information Processing Systems*, I. Guyon, U. V. Luxburg, S. Bengio, H. Wallach, R. Fergus, S. Vishwanathan, and R. Garnett, Eds., Long Beach, USA, Dec. 2017, pp. 5998–6008.
- [19] D. B. Paul and J. M. Baker, "The Design for the Wall Street Journal-based CSR Corpus," in *Proc. Workshop on Speech and Natural Language*, New York, USA, Feb. 1992, pp. 357–362.
- [20] D. Diaz-Guerra, A. Miguel, and J. R. Beltran, "gpuRIR: A python library for room impulse response simulation with GPU acceleration," *Multi-media Tools and Applications*, vol. 80, no. 4, pp. 5653–5671, Feb. 2021.
- [21] J. Le Roux, S. Wisdom, H. Erdogan, and J. R. Hershey, "SDR – Half-baked or Well Done?" in *Proc. IEEE International Conference on Acoustics, Speech and Signal Processing (ICASSP)*, Brighton, UK, May 2019, pp. 626–630.
- [22] H. Erdogan, J. R. Hershey, S. Watanabe, and J. Le Roux, "Phase-Sensitive and Recognition-Boosted Speech Separation Using Deep Recurrent Neural Networks," in *Proc. IEEE International Conference on Acoustics, Speech and Signal Processing (ICASSP)*, Brisbane, Queensland, Australia, Apr. 2015, pp. 708–712.
- [23] Y. Luo and N. Mesgarani, "Conv-TasNet: Surpassing Ideal Time-Frequency Magnitude Masking for Speech Separation," *IEEE/ACM Transactions on Audio, Speech, and Language Processing*, vol. 27, no. 8, pp. 1256–1266, Aug. 2019.
- [24] A. Rix, J. Beerends, M. Hollier, and A. Hekstra, "Perceptual Evaluation of Speech Quality (PESQ) - A New Method for Speech Quality Assessment of Telephone Networks and Codecs," in *Proc. IEEE International Conference on Acoustics, Speech and Signal Processing (ICASSP)*, Salt Lake City, USA, May 2001, pp. 749–752.
- [25] E. Vincent, R. Gribonval, and C. Fevotte, "Performance measurement in blind audio source separation," *IEEE Transactions on Audio, Speech, and Language Processing*, vol. 14, no. 4, pp. 1462–1469, Jul. 2006.